Heat and Technology
Vol. 32, n. 1-2, 2014

INFLUENCE OF THERMAL RADIATION ON NATURAL CONVECTION BOUNDARY LAYER FLOW OF A NANOFLUID PAST A VERTICAL PLATE WITH UNIFORM HEAT FLUX

Machireddy Gnaneswara Reddy
Department of Mathematics, Acharya Nagarjuna University Campus, Ongole,
A.P. (India) – 523 001
E-Mail: mgrmaths@gmail.com

ABSTRACT

In this analysis, the boundary layer flow and heat and mass transfer over a vertical plate due to a nanofluid with the effects of thermal radiation and uniform heat flux have been investigated. The transport equations used in the analysis took into account the effect of Brownian motion and thermophoresis parameters. Similarity transformation is used to convert the governing non-linear boundary-layer equations into coupled higher order non-linear ordinary differential equations. These equations are numerically solved using fourth order Runge–Kutta method along with shooting technique. An analysis has been carried out to elucidate the effects of governing parameters corresponding to various physical conditions. The dimensionless skin friction increases as the Prandtl number, but decreases as the buoyancy ratio parameter and radiation parameter increases. The reduced Nusselt number increases as the Prandtl number and radiation parameter increase. Comparison with published results is presented.

Keywords: Thermal radiation, Brownian motion, Thermophoresis, Nanofluid, vertical plate.

NOMENCLATURE

C	nanoparticle volume fraction
C_w	nanoparticle volume fraction at the plate (wall)
C_∞	nanoparticle volume fraction at large values of y
D_B	Brownian diffusion coefficient
D_T	thermophoretic diffusion coefficient
$f(\eta)$	dimensionless stream function
g	acceleration due to gravity
k	effective thermal conductivity of nanofluid
k_e	the mean absorption coefficient
k_p	thermal conductivity of nanoparticles
k_f	thermal conductivity of base fluid
Le	Lewis number
N	radiation parameter
Nb	Brownian motion parameter
Nr	buoyancy ratio
Nt	thermophoresis parameter
Nu_x	local Nusselt number
Pr	Prandtl number
p	pressure
q_r	radiative heat flux
q_m''	wall mass flux
q_w''	wall heat flux
Ra_x	local Rayleigh number
Sh_x	local Sherwood number
T	local fluid temperature
T_w	wall surface temperature
T_∞	ambient temperature
u, v	velocity components along x and y directions
x	coordinate along the plate
y	coordinate normal to the plate.

Greek symbols

α	thermal diffusivity
β	volumetric thermal expansion coefficient of the base fluid
σ_s	the Stefan-Boltzmann constant
η	similarity variable
μ	absolute viscosity of the base fluid
ν	kinematic viscosity of the fluid
ρ_f	fluid density
ρ_p	nanoparticle mass density
$(\rho c)_f$	heat capacity of the fluid
$(\rho c)_p$	effective heat capacity of the nanoparticle material
τ	ratio between the effective heat capacity of the nanoparticle material and heat capacity of the fluid
θ	dimensionless temperature
ϕ	dimensionless nanoparticle concentration
ψ	stream function

1. INTRODUCTION

Convective heat transfer in nanofluids is a topic of major contemporary interest in the heat transfer research community. The word "nanofluid" coined by Choi [1] describes a liquid suspension containing ultra-fine particles (diameter less than 50 nm). With the rapid advances in nano manufacturing, many inexpensive combinations of liquid/particle are now available. These include particles of metals such aluminum, copper, gold, iron and titanium or their oxides. The base fluids used are usually water, ethylene glycol, toluene and oil. Experimental studies e.g. [2-7] show that even with the small volumetric fraction of nanoparticles (usually less than 5%), the thermal conductivity of the base liquid can be enhanced by 10-50%. The enhanced thermal conductivity of a nanofluid together with the thermal dispersion of particles and turbulence induced by their motion contributes to a remarkable improvement in the convective heat transfer coefficient. This feature of nanofluids make them attractive for use in applications such as advanced nuclear systems [8] and cylindrical heat pipes [9]. The literature on the thermal conductivity and viscosity of nanofluids has been reviewed by Trisaksri and Wongwises [10],Wang and Mujumdar [11], Eastman et al. [12], and Kakac and Pramuanjaroenkij [13], among several others. These reviews discuss in detail the preparation of nanofluids, theoretical and experimental investigations of thermal conductivity and viscosity of nanofluids, and the work done on convective transport in nanofluids. A benchmark study of thermal conductivity of nanofluids has been published by Buongiorno et al. [14].

Khanafer et al. [15] analyzed the two-dimensional natural convective flow of a nanofluid in an enclosure and found that for any given Grashof number, the heat transfer rate increased as the volume fraction of nanoparticles increased. Kim et al. [16] introduced a new friction factor to describe the effect of nanoparticles on the convective instability and the heat transfer characteristics of the base fluid. Tzou [17] considered thermal instability of nanofluids in natural convection and concluded that the higher turbulence triggered by the nanoparticles prompted higher heat transfer coefficient than the effect of enhanced thermal conductivity. Contrary to the observations in [15], Putra et al. [18] and Wen and Ding [19] found that the heat transfer coefficient decreases, not increases, with the increase in particle concentration. The difference in conclusions of the analytical studies of Khanafer et al. [15] and Kim et al. [16] and experimental works of Putra et al. [18] andWen and Ding [19] may be due to the assumptions made in [15,16,26,29] in developing the analytical models. In a more recent paper, Abu-Nada et al. [20] studied the effect of variable thermal conductivity and variable viscosity on heat transfer in awatere Al_2O_3 nanofluid confined in an enclosure. Khan and Aziz [21] to investigate the boundary layer flow of a nanofluid past a vertical surface with a constant heat flux.

Radiative flows are encountered in countless industrial and environmental processes e.g., heating and cooling chambers, fossil fuel combustion and energy processes, evaporation from large open water reservoirs, astrophysical flows and solar power technology. However, the thermal radiation heat transfer effects on different flows are very important in high temperature processes and space technology. Gnaneswara Reddy [22] analyzed mass transfer effects on the unsteady MHD radiative convective flow of a micropolar fluid past a vertical porous plate with variable Heat and mass fluxes. Thermophoresis effects on MHD combined heat and mass transfer in two-dimensional flow over an inclined radiative isothermal permeable surface was investigated by M. Gnaneswara Reddy [23,25]. Very Recently, M. Gnaneswara Reddy [24] studied the influence of magnetohydrodynamic and thermal radiation boundary layer flow of a nanofluid past a stretching sheet.

But so far, no attempt has been made to analyze the natural convective boundary layer flow of a nanofluid past a vertical plate with uniform heat flux in the presence of heat radiation and hence we have considered the problem of this kind. A similarity solution is derived and used to predict the heat and mass transfer characteristics of the flow.

2. FORMULATION OF THE PROBLEM

Consider the two-dimensional (x, y) natural convection boundary layer flow over a vertical plate. The physical model for this problem is shown in Fig. 1. Although a single boundary layer is shown in Fig. 1 to avoid congestion, there are three distinct boundary layers over the plate, namely, a hydrodynamic (velocity) boundary layer, a thermal (temperature) boundary layer, and a concentration (volume fraction of nanoparticles) boundary layer. The nanofluid in contact with the plate has a volumetric nanoparticle fraction C_w at the plate $(y=0)$ and a value C_∞ at large values of y $(y \to \infty)$. The plate has a constant heat flux q_w'' imposed at its surface.

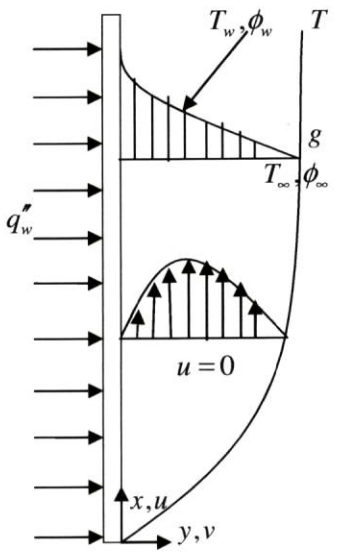

Fig.1. Physical model of boundary layer flow over a vertical plate.

The governing equations for the conservation of total mass, momentum, thermal energy, and nanoparticles derived by Kuznetsov and Nield [27] may be written as

$$\frac{\partial u}{\partial x}+\frac{\partial v}{\partial y}=0 \qquad (1)$$

$$\frac{\partial p}{\partial x}=\mu\frac{\partial^2 u}{\partial y^2}-\rho_f\left(u\frac{\partial u}{\partial x}+v\frac{\partial u}{\partial y}\right)+\left[\begin{matrix}(1-C_\infty)\rho_{f\infty}\beta(T-T_\infty)\\-(\rho_p-\rho_{f\infty}g(C-C_\infty))\end{matrix}\right] \quad (2)$$

$$\frac{\partial T}{\partial x}+v\frac{\partial T}{\partial y}=\alpha\nabla^2 T-\frac{1}{(\rho c)_f}\frac{\partial q_r}{\partial y}+\tau\left[D_B\frac{\partial C}{\partial y}\frac{\partial T}{\partial y}+\left(\frac{D_T}{T_\infty}\right)\frac{\partial^2 T}{\partial y^2}\right] \quad (3)$$

$$u\frac{\partial C}{\partial x}+v\frac{\partial C}{\partial y}=D_B\left(\frac{\partial^2 C}{\partial x^2}+\frac{\partial^2 C}{\partial y^2}\right)+\left(\frac{D_T}{T_\infty}\right)\left(\frac{\partial^2 T}{\partial x^2}+\frac{\partial^2 T}{\partial y^2}\right) \quad (4)$$

The appropriate boundary conditions for the physical problem under consideration are given by

$$u=0, v=0, -k\frac{\partial T}{\partial y}=q_w'', C=C_w \ at \ y=0$$
$$u\to 0,\ T\to T_\infty,\ C\to C_\infty \ \ as \ \ y\to\infty \quad (5)$$

By using the Rosseland approximation (Brewster [28]), the radiative heat flux q_r is given by

$$q_r=-\frac{4\sigma_s}{3k_e}\frac{\partial T'^4}{\partial r} \quad (6)$$

where σ_s is the Stefan-Boltzmann constant and k_e - the mean absorption coefficient. It should be noted that by using the Rosseland approximation, the present analysis is limited to optically thick fluids. If the temperature differences within the flow are sufficiently small, then Equation (6) can be linearized by expanding T'^4 into the Taylor series about T_∞', which after neglecting higher order terms takes the form

$$T'^4\cong 4T_\infty'^3T'-3T_\infty'^4 \quad (7)$$

In view of Equations (6) and (7), Equation (3) reduces to

$$\frac{\partial T}{\partial x}+v\frac{\partial T}{\partial y}=\alpha\nabla^2 T+\frac{16\sigma_s T_\infty^3}{3k_e(\rho c)_f}\nabla^2 T+\tau\left[D_B\frac{\partial C}{\partial y}\frac{\partial T}{\partial y}+\left(\frac{D_T}{T_\infty}\right)\frac{\partial^2 T}{\partial y^2}\right] \quad (8)$$

Introducing stream function $\psi(x,y)$ defined by

$$u=\frac{\partial\psi}{\partial y} \text{ and } v=-\frac{\partial\psi}{\partial x} \quad (9)$$

so the continuity equation, Eq. (1) is identically satisfied.

Let us consider the similarity transformations for the constant heat flux boundary condition. The following quantities are introduced to transform Eqs. (2), (8) and (4) into ordinary differential equations.

$$\eta=\frac{y}{x}Ra_x^{1/4},\ \psi=\alpha Ra_x^{1/4}f(\eta),\ \theta(\eta)=\frac{T-T_\infty}{(q''x/k)},\ \phi(\eta)=\frac{C-C_\infty}{C_w-C_\infty} \quad (10)$$

with the local Rayleigh number is defined as

$$Ra_x=\frac{(1-C_\infty)g\beta(q''x/k)x^3}{\nu\alpha} \quad (11)$$

After some algebraic manipulation, the momentum, energy, and volume fraction equations are obtained the following three coupled, nonlinear ordinary differential equations

$$f'''+\frac{1}{\Pr}(ff''-f'^2)+\theta-Nr\phi=0 \quad (12)$$

$$\left(1+\frac{4}{3N}\right)\theta''+Nt\theta'^2+Nb\phi'\theta'+f\theta'-f'\theta=0 \quad (13)$$

$$\phi''+\frac{Nt}{Nb}\theta''+Lef\phi'=0 \quad (14)$$

The corresponding boundary conditions take the form

$$f=0,\ f'=0,\ \theta'=-1,\ \phi=1 \ at \ \ \eta=0$$
$$f'\to 0,\ \theta\to 0,\ \phi\to 0 \ \ as \ \eta\to\infty \quad (15)$$

where primes denote differentiation with respect to η and are defined as follows

$$Nr=\frac{(\rho_p-\rho_f)(C_w-C_\infty)}{\rho_f\beta(1-C_w)(q_w''x/k)},\ N=\frac{kk_e}{4\sigma_s T_\infty^3},$$
$$Nb=\frac{\tau D_B(C_w-C_\infty)}{\alpha},\ \Pr=\frac{\nu}{\alpha},$$
$$Nt=\frac{\tau D_T(q_w''x/k)}{\alpha T_\infty},\ Le=\frac{\alpha}{D_B}$$

The quantities of practical interest, in this study, are the dimensionless skin friction given by $f''(0)$, the local Nusselt number Nu_x and the Sherwood number Sh_x which are defined as

$$f''(0)=\frac{\tau_w x^2}{\mu\alpha Ra_x^{3/4}} \quad (16)$$

$$Nu_x=\frac{xq_w''}{k(T_w-T_\infty)} \quad (17)$$

$$Sh_x=\frac{xq_m''}{D_B(\phi_w-\phi_\infty)} \quad (18)$$

where q_w'' and q_m'' are the wall heat and mass fluxes, respectively, and τ_w is the wall shear stress. Following Kuznetsov and Nield [27], the reduced local Nusselt number Nur and reduced local Sherwood number Shr can be introduced and represented as follows

$$Nur=Ra_x^{1/4}Nu_x=\frac{1}{\theta(0)} \quad (19)$$

$$Shr=Ra_x^{1/4}Sh_x=-\phi'(0) \quad (20)$$

3. NUMERICAL SOLUTION

The set of nonlinear ordinary differential equations (12) - (14) with boundary conditions (15) have been solved by using the Runge-Kutta fourth order along with Shooting method. First of all, higher order non-linear differential Equations (12) - (14) are converted into simultaneous linear differential equations of first order and they are further transformed into initial value problem by applying the shooting technique. The resultant initial value problem is solved by employing Runge-Kutta fourth order technique. The step size $\Delta\eta = 0.01$ is used to obtain the numerical solution with five decimal place accuracy as the criterion of convergence.

4. RESULTS AND DISCUSSION

The numerical solutions are obtained for velocity, temperature and concentration profiles for different values of governing parameters. The obtained results are displayed through graphs Figs. 2–16 for dimensionless velocity, dimensionless temperature and dimensionless Nanoparticle concentration profiles, respectively.

In the present study following default parameter values are adopted for computations: $\Pr = 2.0$, $Nr = 0.2$, $N = 2.0$, $Nt = 0.2$, $Nb = 0.4$ and $Le = 2.0$. All graphs therefore correspond to these values unless specifically indicated on the appropriate graph.

In order to test the accuracy of our results, we have compared our results with those of Khan and Aziz [21] when we neglect the effects of N. The comparison shows good agreement as presented in Fig. 2.

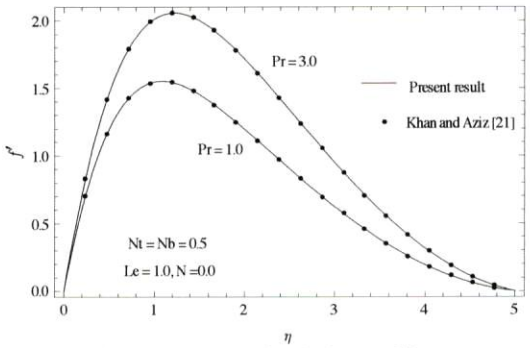

Fig.2. Comparison of velocity profiles.

Figs. 3, 4 and 5 display the effect of thermal radiation parameter N on the velocity, temperature and concentration (volume fraction of nanoparticles) profiles. The radiation parameter defines the relative contribution of conduction heat transfer to thermal radiation transfer. It can be seen that an in increase in N leads to a decrease in the velocity. At a particular value of N, the temperature decreases with accompanying decreases in the thermal boundary layer thickness by increasing the values of $\Pr$ whereas the nanoparticle volume fraction profiles are not significant with increase of N.

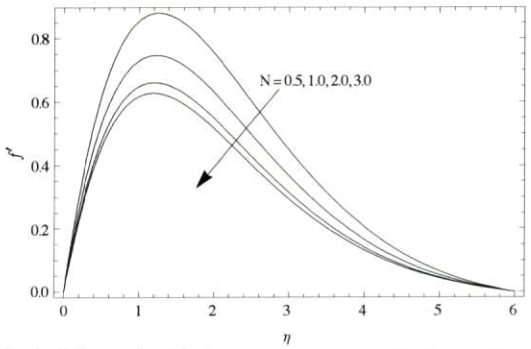

Fig.3. Effect of radiation parameter on velocity profiles.

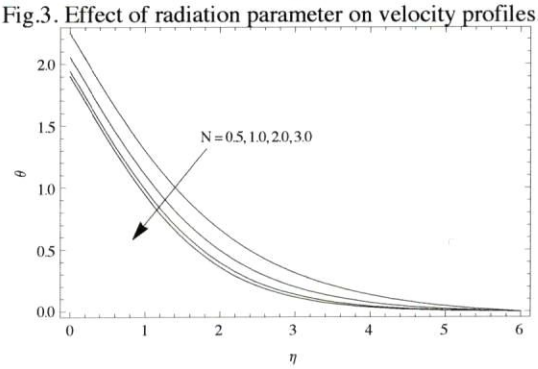

Fig.4. Effect of radiation parameter on temperature profiles.

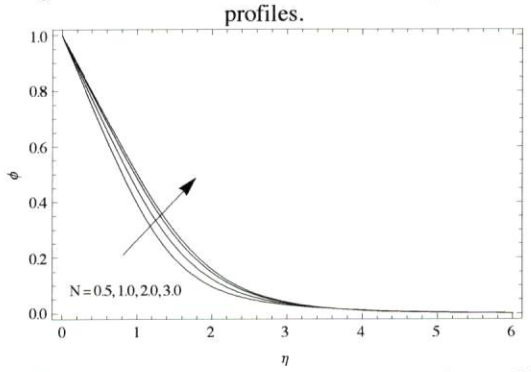

Fig.5. Effect of radiation parameter on concentration profiles.

Further, it is obvious that for a given $\Pr$, the temperature is decreased with an increase in N. This result can be explained by the fact that a decrease in the values of $\left(N = \dfrac{kk_e}{4\sigma_s T_\infty^3} \right)$ for given k_e and T_∞ means a decrease in the Rosseland radiation absorptive k_e. According to Eqs. (2) - (4), the divergence of the radiative heat flux $\dfrac{\partial q_r}{\partial y}$ increases as k decreases which in turn increases the rate of radiative heat transferred to the nanofluid and hence the fluid temperature decreases. In view of this explanation, the effect of radiation becomes more significant as $N \to 0$ $(N \neq 0)$ and can be neglected when $N \to \infty$. It is noticed from the figure that the temperature decreases with the increasing value of the radiation parameter N. The effect of radiation parameter N is to reduce the temperature significantly in the flow region. The increase in radiation parameter means the release of heat

energy from the flow region and so the fluid temperature decreases as the thermal boundary layer thickness becomes thinner. Also, it observed that the concentration is increased with an increase in N .

Figures 6, 7 and 8 illustrate the velocity, temperature and concentration profiles for different values of the Prandtl number Pr. The local dimensionless velocity is seen to increase with an increase in the Prandtl number $\mathbf{Pr}$. As the Prandtl number increases, the hydrodynamic boundary layer thickness increases and as a result, the local velocity also increases. Unlike the hydrodynamic boundary layer, the thermal boundary layer thickness decreases with an increase in Prandtl number. This shows that the effect of Prandtl number on a nanofluid thermal boundary layer is similar to its effect on a regular fluid thermal boundary layer. It is seen that that the concentration is decreased with an increase in $\mathbf{Pr}$.

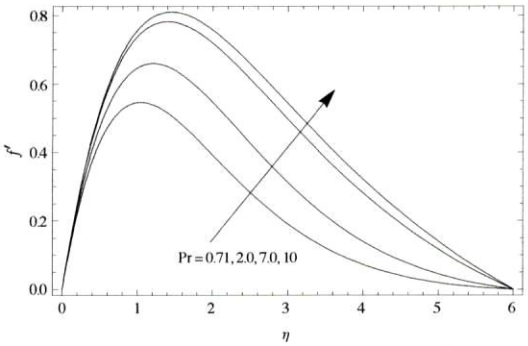

Fig.6. Effect of Prandtl number on velocity profiles.

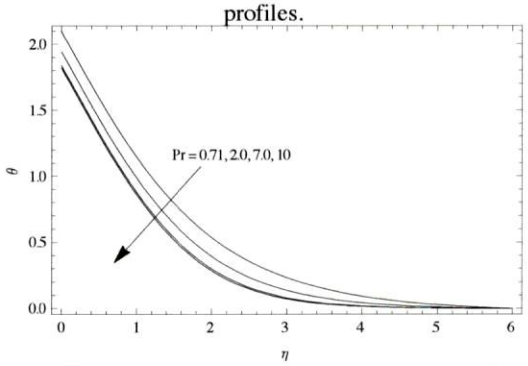

Fig.7. Effect of Prandtl number on temperature profiles.

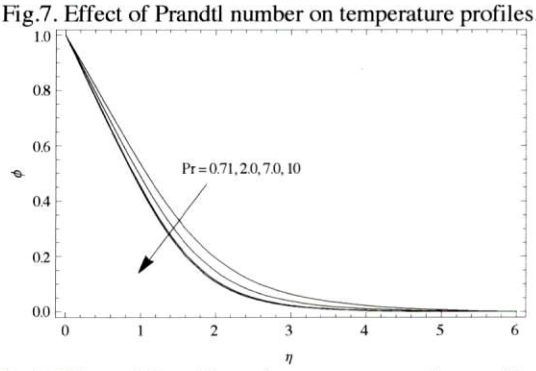

Fig.8. Effect of Prandtl number on concentration profiles.

Fig. 9 reveals the influences of buoyancy-ratio parameter on the velocity profiles. The local dimensionless velocity is seen to decrease with an increase in the buoyancy-ratio parameter Nr .

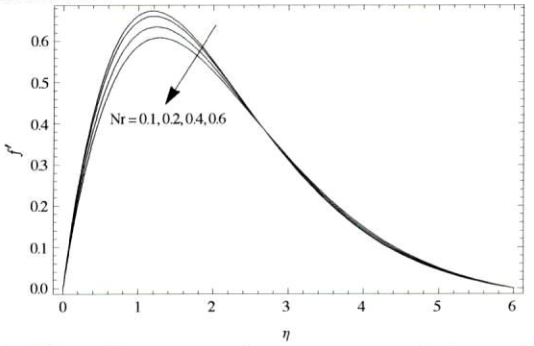

Fig.9. Effect of buoyancy-ratio parameter on velocity profiles.

The effects of Brownian motion and the thermophoresis parameters on dimensionless temperature profiles when $(Nb = Nt)$ are shown in Fig. 10. It is noticed that as thermophoesis parameter increases the thermal boundary layer thickness increases and the temperature gradient at the surface decrease (in absolute value) as both Nb and Nt increase. It can be seen that the local temperature rises as the Brownian motion and thermophoresis parameters increase. A similar conclusion was derived by Khan and Pop [21] in their study of boundary layer flow of a nanofluid past over a vertical plate. However, contrary to the present observation, Kuznetsov and Nield [27] found the temperature profiles to be rather insensitive to the variation of Brownian motion and thermophoresis parameters.

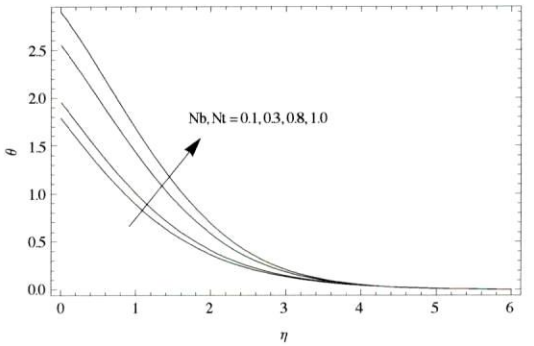

Fig.10. Effects of Brownian motion and the thermophoresis parameters on temperature profiles.

Fig.11. illustrates the influence of Brownian motion and thermophoresis on the nanoparticle concentration profiles when $(Nb = Nt)$. As the values of Brownian motion parameter increase, the concentration boundary layer thickness is decreasing. Furthermore, the magnitude of concentration gradient on the surface of a plate increases as the values of Nb increase. The influence of thermophoresis parameter on concentration profile graph is monotonic, i.e. as the values of Nt parameter increase, the concentration boundary layer thickness is also increasing. Moreover, it is possible to recognize from the graph that the magnitude of concentration gradient on the surface of a sheet decreases as the values Nt increase. The local concentration decreases

markedly as the Brownian motion and thermophoresis parameters increase from 0.1 to 1.0.

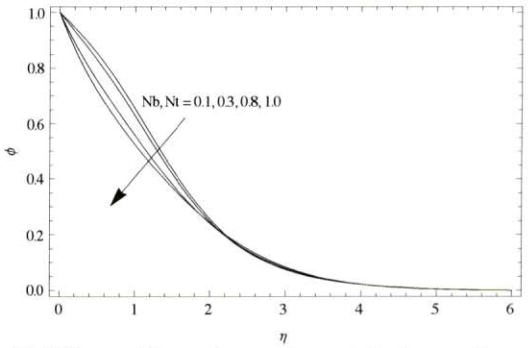

Fig.11. Effects of Brownian motion and the thermophoresis parameters on concentration profiles.

Fig. 12 shows the influence of Lewis number Le on the nanoparticle concentration profiles. As it is noticed from Fig. 12, as Lewis number increases the concentration graph decreases and the concentration boundary layer thickness decreases. This is probably due to the fact that mass transfer rate increases as Lewis number increases. It also reveals that the concentration gradient at surface of the plate increases. Moreover, the concentration at the surface of a plate decreases as the values of Le increase.

The effect of buoyancy-ratio parameter on the dimensionless skin friction i.e. $f''(0)$ are shown in Fig. 13.

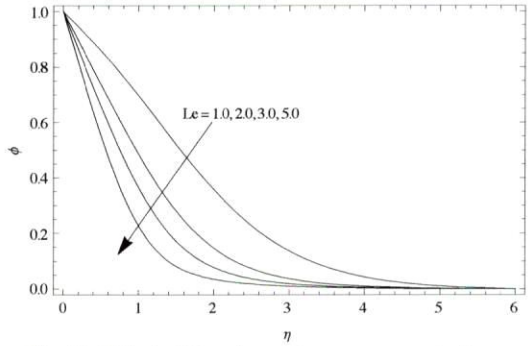

Fig.12. Effect of Lewis number on concentration profiles.

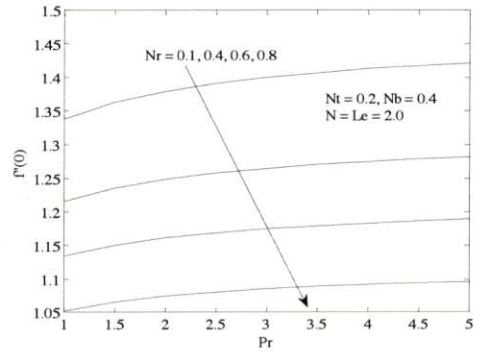

Fig.13. Effect of buoyancy-ratio parameter on skin friction.

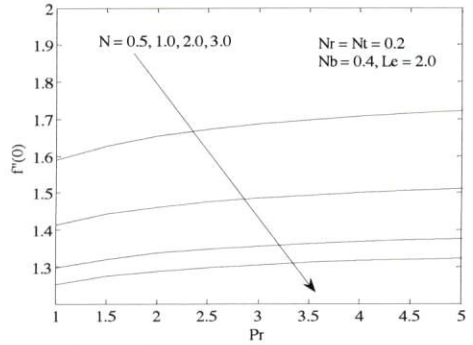

Fig.14. Effect of radiation parameter on skin friction.

It is seen that the skin friction increases with the Prandtl number, but the curves flatten out for large values of the Prandtl number. Also, the skin friction decreases with an increase in the buoyancy parameter.

Fig. 14 illustrates the variation of radiation on the dimensionless skin friction. The graph shows that the skin friction decreases as N parameters increase.

The reduced local Nusselt number Nur is plotted against the Prandtl number in Fig.15 for several values of the radiation parameter. It can be seen that the reduced local Nusselt number Nur increases as the Prandtl number increases. As the values of thermal radiation parameter N increase, the local Nusselt number increases.

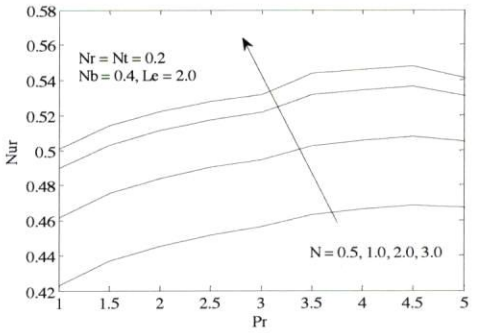

Fig.15. Effect of radiation parameter on reduced Nusselt number.

The reduced local Sherwood number Shr is plotted against the Prandtl number in Fig.16 for several values of Lewis number. As the values of Lewis number increases, the values of Shr increases.

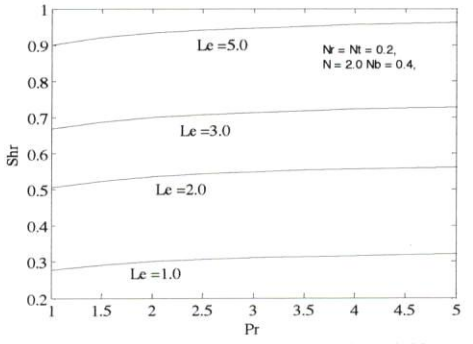

Fig.16. Effect of Lewis number on reduced Sherwood number.

5. CONCLUSIONS

The main findings of the study are summarized as follows:

1. Temperature decreases with the increasing value of the radiation parameter N .
2. Thermal boundary layer thickness increases with an increase in Prandtl number Pr.
3. The thermophoesis parameter increases the thermal boundary layer thickness increases and the temperature gradient at the surface decrease (in absolute value) as both Nb and Nt increase.
4. The dimensionless skin friction increases as the Prandtl number, but decreases as the buoyancy ratio parameter and radiation parameter increases.
5. The reduced Nusselt number increases as the Prandtl number and radiation parameter increase.

ACKNOWLEDGEMENT

The author wish to express their very sincere thanks to referees for their valuable comments and suggestions for the improvement of the manuscript.

REFERENCES

1. S.U.S. Choi, Enhancing Thermal Conductivity of Fluids with Nanoparticles (1995) Developments and Applications of Non-Newtonian Flows, FED-231/ MD-vol.66, 99-105.
2. H. Masuda, A. Ebata, K. Teramea, N. Hishinuma, Altering the thermal conductivity and viscosity of liquid by dispersing ultra-fine particles, Netsu Bussei 4 (4) (1993) 227-233.
3. S.Das, Temperature dependence of thermal conductivity enhancement for nanofluids, J. Heat Transfer 125 (2003) 567-574.
4. B.C. Pak, Y. Cho, Hydrodynamic and heat transfer study of dispersed fluids with submicron metallic oxide particles, Exp. Heat Transfer 11 (1998) 151-170.
5. Y. Xuan, Q. Li, Investigation on convective heat transfer and flow features of nanofluids, J. Heat Transfer 125 (2003) 151-155.
6. J.A. Eastman, SU.S. Choi, S. Li, W. Yu, L.J. Thompson, Anomalously increased effective thermal conductivity of ethylene glycol-based nanofluids containing copper nanoparticles, Appl. Phys. Lett. 78 (6) (2001) 718-720.
7. H.A. Minsta, G. Roy, C.T. Nguyen, D. Doucet, New temperature dependent thermal conductivity data for water-based nanofluids, Int. J. Thermal Sci. 48 (2009) 363-371.
8. J. Buongiorno, L.-W. Hu, Nanofluid Coolants for Advanced Nuclear Power Plants (2005) Paper No. 5705, Proceedings of ICAPP 2005, Seoul, May 15-19.
9. K.N. Shukla, A. Brusty Solomon, B.C. Pillai, Mohammed Ibrahim, Thermal performance of cylindrical heat pipe using nanofluids, J. Thermophysics Heat Transfer 24 (2010) 796-802.
10. V. Trisaksri, S. Wongwises, Critical review of heat transfer characteristics of nanofluids, Renewable Sustainable Energy Rev. 11 (2007) 512-523.
11. X.-Q. Wang, A.S. Mujumdar, Heat transfer characteristics of nanofluids: a review, Int. J. Thermal Sci. 46 (2007) 1-19.
12. J.A. Eastman, S.R. Phillpot, S.U.S. Choi, P. Keblinski, Thermal transport in nanofluids, Annu. Rev. Mater. Res. 34 (2004) 219-246.
13. S. Kakac, A. Pramaumjaroenkij, Review of convective heat transfer enhancement with nanofluids, Int. J. Heat Mass Transfer 52 (2009) 3187-3196.
14. J. Boungiorno, et al., A benchmark study of thermal conductivity of nanofluids, J. Appl. Phys. 106 (2009) Paper 094312.
15. K. Khanafer, K. Vafai, M. Lightstone, Buoyancy-driven heat transfer enhancement utilizing nanofluids, Int. J. Heat Mass Transfer 46 (2003) 3639-3653.
16. J. Kim, Y.T. Kang, C.K. Choi, Analysis of convective instability and heat transfer characteristics of nanofluids, Phys. Fluids 16 (2004) 2395-2401.
17. D.Y. Tzou, Thermal stability of nanofluids in natural convection, Int. J. Heat Mass Transfer 51 (2008) 2967-2979.
18. N. Putra, W. Roetzel, S.K. Das, Natural convection in nanofluids, Heat and Mass Transfer 39 (8-9) (2003) 775-784.
19. D. Wen, Y. Ding, Formulation of nanofluids for natural convective heat transfer application, Int. J. Heat Fluid Flow 26 (6) (2005) 855-864.
20. E. Abu-Nada, Z. Masoud, H.F. Oztop, A. Campo, Effect of nanofluid variable properties on natural convection in enclosure, Int. J. Thermal Sci. 49 (2010) 479-491.
21. W.A. Khan, I. Aziz, Natural convection flow of a nanofluid over a vertical plate with uniform surface heat flux, Int. J. Thermal Sci. 50 (2011) 1207-1214.
22. M. Gnaneswara Reddy, Mass transfer effects on unsteady MHD radiative convection flow of micropolar fluid past a vertical porous plate with variable heat and mass fluxes, Journal of Engineering Physics and Thermophysics, 86(2) (2013) 406-415.
23. M. Gnaneswara Reddy, Thermophoresis effects on MHD combined heat and mass transfer in two-dimensional flow over an inclined radiative isothermal permeable surface, ACTA TECHNICA, 58 (1) (2013) 41-58.
24. M. Gnaneswara Reddy, Influence of magnetohydrodynamic and thermal radiation boundary layer flow of a nanofluid past a stretching sheet, J. Sci. Res. **6** (2), 257-272 (2014).
25. M. Gnaneswara Reddy, Effects of thermophoresis, viscous dissipation and joule heating on steady MHD heat and mass transfer flow over an inclined radiative isothermal permeable surface with variable thermal conductivity, Int. J. Heat and Technology, 30 (1), 2012, pp. 99-110.
26. M.M. Rahman, A. Aziz, Heat transfer in water based nanofluids (TiO2-H2O, Al2O3-H2O and Cu-H2O) over a stretching cylinder, Int. J. Heat and Technology, 30 (2), 2012, pp.31-42.
27. A.V. Kuznetsov, D.A. Nield, Natural convective boundary-layer flow of a nanofluid past a vertical plate, Int. J. Thermal Sci. 49 (2010) 243-247.
28. Brewster M.Q. (1992), Thermal radiative transfer and properties, John Wiley & Sons, New York.
29. Daniele De Wrachien, Giulio Lorenzini, Marco Medici, Water droplet and aerial path in irrigation systems: classical and quantum termofluidynamical approaches and numerical approximation methods Int.J. OF HEAT &TECH, vol31 2013, pp. 81-86